Calcium increases endocytotic vesicle size and accelerates membrane fission in insulin-secreting INS-1 cells

Patrick E. MacDonald[1,2,*], Lena Eliasson[1] and Patrik Rorsman[1,2]

[1]Division of Diabetes, Metabolism and Endocrinology, Lund University, 221 84 Lund, Sweden
[2]Oxford Centre for Diabetes, Endocrinology and Metabolism, Churchill Hospital, Headington, Oxford, OX3 7LJ, UK
*Author for correspondence (e-mail: pmacdonald@bcell.org)

Accepted 9 September 2005
Journal of Cell Science 118, 5911-5920 Published by The Company of Biologists 2005
doi:10.1242/jcs.02685

Summary

In many cells, endocytotic membrane retrieval is accelerated by Ca^{2+}. The effect of Ca^{2+} on single endocytotic vesicles and fission pore kinetics was examined by measuring capacitance and conductance changes in small membrane patches of insulin-secreting INS-1 cells. In intact cells, elevation of Ca^{2+} by glucose stimulation induced a 1.8-fold increase in membrane internalisation. This surprisingly resulted from an increased unitary capacitance of endocytotic vesicles whereas the frequency of endocytosis was unaltered. This effect of glucose was prevented by inhibition of L- or R-type Ca^{2+} channels. Extracellular (pipette) Ca^{2+} was found to regulate endocytotic vesicle capacitance in a bimodal manner. Vesicle capacitance was increased at intermediate Ca^{2+} (2.6 mM), but not at high Ca^{2+} (10 mM). Similar results were obtained upon direct application of 100 nM and 0.5 mM Ca^{2+} to the intracellular surface of inside-out excised membrane patches, and in these experiments the increase in vesicle capacitance was prevented by the calcineurin inhibitor deltamethrin. Endocytotic fission pore kinetics were accelerated by Ca^{2+} in both the intact cells and isolated membrane patches; however, the effect in this case was neither bimodal nor deltamethrin sensitive. Membrane retrieval can therefore be upregulated by a Ca^{2+}-dependent increase in endocytotic vesicle size and acceleration of membrane fission in insulin-secreting INS-1 cells.

Key words: Insulin, INS-1, Calcium, Endocytic vesicle, Membrane fission

Introduction

Regulated exocytosis is coupled to endocytotic membrane retrieval and, in many cells, endocytosis is Ca^{2+} dependent. The molecular machinery mediating Ca^{2+}-dependent endocytosis is best characterized in the context of synaptic vesicle recycling (Jarousse and Kelly, 2001; Murthy and De Camilli, 2003; Wu, 2004), where the Ca^{2+}-sensitive phosphatase calcineurin targets numerous essential endocytotic proteins (Cousin and Robinson, 2001). Calcineurin is therefore considered the Ca^{2+} sensor for endocytosis (Bauerfeind et al., 1997; Liu et al., 1994; Marks and McMahon, 1998). Endocrine secretory cells release peptides and small molecules through the regulated exocytosis of large dense-core and synaptic-like vesicles. Endocytosis in adrenal chromaffin cells is dependent on Ca^{2+} and calmodulin (Artalejo et al., 1995; Artalejo et al., 1996), although there are distinct calcineurin-dependent and -independent pathways (Chan and Smith, 2001; Engisch and Nowycky, 1998). In pancreatic β-cells, exocytosis is stimulated by glucose-dependent Ca^{2+} influx, and accordingly endocytosis is upregulated by glucose (Orci et al., 1973) and Ca^{2+} (Eliasson et al., 1996), and may also involve a calcineurin-dependent step (Hoy et al., 2002a).

Despite recent advances in understanding the role of Ca^{2+} as a regulator of membrane retrieval, little is known about the effects of Ca^{2+} at the single vesicle level. This is at least in part owing to the difficulty in measuring small unitary endocytotic events. The fusion and fission of single vesicles is associated with discrete changes in the capacitance of small membrane patches (Neher and Marty, 1982). Single endocytotic vesicles with capacitances in the low atto-Farad (aF) range (<100 nm diameter) have been observed previously in membrane patches (Chowdhury et al., 2002; Dernick et al., 2003; Henkel et al., 2001; Kreft and Zorec, 1997; Lollike et al., 1995; Rosenboom and Lindau, 1994; Schwake et al., 2002). However, none of these studies has examined the role of Ca^{2+} in endocytosis. Additionally, analysis of transient increases in patch conductance allows examination of the kinetics of membrane fission during endocytosis (Dernick et al., 2003; Rosenboom and Lindau, 1994). Cell-attached patch capacitance measurements are therefore ideally suited to investigate the regulation of endocytosis and membrane fission at the single vesicle level.

Here, we have examined endocytosis of single vesicles in cell-attached and inside-out excised membrane patches from INS-1 β-cells, which retain many features of primary β-cells and secrete insulin in response to glucose stimulation. Membrane internalisation was upregulated by glucose and Ca^{2+}, and this surprisingly resulted from an increase in endocytotic vesicle size. Also, Ca^{2+} accelerated the kinetics of membrane fission. Calcineurin is implicated in the Ca^{2+}-

dependent increase in vesicle size; however, the effect on fission pore kinetics was independent of calcineurin. We propose that, in insulin-secreting INS-1 cells, Ca^{2+} can couple endocytosis to exocytosis in part by increasing endocytotic vesicle size and accelerating the kinetics of fission.

Materials and Methods

Cells and cell culture

INS-1 cells, a gift from C. Wollheim (University Medical Center, Geneva, Switzerland), were cultured at 37°C and 5% CO_2 in RPMI-1640 media supplemented with 10% FBS, 100 units/ml penicillin G sodium, 100 μg/ml streptomycin sulphate and 50 μM β-mercaptoethanol. Cells were plated in 35 mm plastic dishes 18-48 hours prior to experiments.

Patch capacitance measurements

Membrane patch capacitance measurements were performed in the cell-attached and excised-patch configurations (Dernick et al., 2003; Lollike and Lindau, 1999) using a sine wave of 18 or 25 kHz and 50 mV rms around 0 mV. The time constant of the lock-in amplifier (SR830, Stanford Research Systems) was 3 ms (24 dB). Patch-pipettes were coated with Sylgard and had an average resistance when fire polished of 2.49±0.04 MΩ for cell-attached and 3.58±0.05 MΩ for excised-patch experiments. Pure capacitance increases produced by pulses of pipette suction were used for on-line phase calibration. Remaining small offsets were corrected off-line (Debus and Lindau, 2000).

For cell-attached experiments, the bath solution contained: 125 mM NaCl, 4 mM KCl, 2 mM EGTA, 1 mM $MgCl_2$, 0 or 10 mM glucose, and 10 mM HEPES at pH 7.2. The pipette solution contained: 125 mM NaCl, 4 mM KCl, 10 or 2.6 or 0 mM $CaCl_2$, 1 mM $MgCl_2$, 13 mM TEA-Cl, and 10 mM HEPES at pH 7.2. When the pipette solution had 0 mM $CaCl_2$, 2 mM EGTA was also included. Isradipine (2 μM, with 0.02% DMSO; Alomone Labs) or SNX-482 (100 nM; Peptide Institute) was included in the pipette solution as indicated. For excised-patch experiments, the pipette solution contained: 120 mM Na-glutamate, 20 mM NaCl, 5 mM KCl, 1 mM $MgCl_2$, 0.5 mM $CaCl_2$ and 10 mM HEPES at pH 7.4. The bath solution was the same, although Ca^{2+} was either absent (with 0.1 mM EGTA), buffered to 100 nM free-Ca^{2+} (1.24 mM $CaCl_2$, 1.11 mM $MgCl_2$ and 2 mM EGTA) or present at 0.5 mM. Calcineurin (0.4 U/ml; Sigma-Aldrich) and calmodulin (100 U/ml; Sigma-Aldrich), or deltamethrin (1 μM with 0.01% DMSO) were added to the bath as indicated. DMSO alone (0.01%) had no effect in six cells. The bath was perfused continuously at 32°C.

Data analysis

The X and Y outputs of the lock-in amplifier reflect the real (Re) and imaginary (Im) conductance components. On-line phase calibration generally resulted in good separation of the Im and Re conductance components. Occasional small phase offsets, observed as step-wise changes in Re upon endocytosis, were corrected off-line prior to further analysis (Debus and Lindau, 2000). When Re is constant (and the phase setting is correct), capacitance changes are reflected by $Im/2\pi f$, where f is the sine wave frequency. However, when Re changes transiently upon a capacitance step, indicating a fission pore, vesicle capacitance (C_v) and pore conductance (G_p) were calculated as described (Lollike and Lindau, 1999). The time constant (τ) of the G_p decrease was determined by fitting to a single exponential decay function and the final conductance before pore closure was averaged over the final 25 ms. Membrane area and vesicle diameter were calculated assuming 9 femto-Farad (fF)/μm^2 as the specific membrane capacitance (MacDonald et al., 2005). The average vesicle diameter was calculated separately following transformation of the capacitance data.

The membrane area internalisation rate (μm^2 $patch^{-1}$ $minute^{-1}$) and event frequency ($patch^{-1}$ $minute^{-1}$) were calculated on a patch-by-patch basis (i.e. by dividing the area or events observed in a given membrane patch by the recording time for that patch). The average patch lifetime was 4.1±0.1 minutes in cell-attached experiments and 3.4±0.2 minutes in excised-patch experiments. Results were extrapolated to the whole cell by dividing patch areas estimated from pipette resistances (Sakmann and Neher, 1995) by the total membrane area calculated from whole-cell INS-1 capacitance (7.73 fF; 858.9 μm^2). Data were compared by ANOVA and multiple comparisons post-test. *P*-values less than 0.05 were considered significant.

Results

Capacitance steps reflecting endocytosis in membrane patches

The INS-1 line is a well-characterised insulin-secreting rat β-cell line (Hohmeier and Newgard, 2004) in which both large dense-core vesicles and synaptic-like vesicles undergo glucose and Ca^{2+}-regulated exocytosis. The mean diameters of these vesicles are 67 and 185 nm, respectively (MacDonald et al., 2005). Measurement of membrane patch capacitance in the cell-attached configuration affords an improved resolution compared with traditional whole-cell measurements (Neher and Marty, 1982). Downward steps in capacitance ($Im/2\pi f$) result from the internalisation of single endocytotic vesicles, whereas the real (Re) component reflects patch conductance (Fig. 1A). Occasionally, an endocytotic event followed an exocytotic event of similar magnitude, reflecting the direct retrieval of an exocytotic vesicle by 'kiss-and-run' (Albillos et al., 1997). These accounted for only a minor fraction of the total endocytosis observed (<2%) and were excluded from the present analysis, and we thus examined only endocytotic events likely to represent the de novo formation of endocytotic vesicles.

The size distribution of endocytotic events under basal conditions (0 mM glucose in the bath; 2.6 mM pipette-Ca^{2+}) is shown in Fig. 1B. Under these conditions, 350 endocytotic events were observed in membrane patches from 41 cells. The mean capacitance of endocytotic vesicles was 150±5 aF, equivalent to a diameter of 70±1 nm and similar in size to synaptic-like microvesicles in these cells (MacDonald et al., 2005). Endocytotic events occurred with a frequency of 1.7±0.4 $patch^{-1}$ $minute^{-1}$ (or 274±69 $cell^{-1}$ $minute^{-1}$). Total membrane internalisation, calculated as the sum of all endocytotic steps in a patch and extrapolated to the whole cell, occurred at an average rate of 4.6±1.2 μm^2 $cell^{-1}$ $minute^{-1}$.

Calcium entry regulates endocytotic vesicle size

Glucose stimulation depolarises pancreatic β-cells, resulting in Ca^{2+} entry through voltage-dependent Ca^{2+} channels and exocytosis. Endocytosis is also Ca^{2+} dependent in many cells, and in β-cells is upregulated by both glucose stimulation (Orci et al., 1973) and Ca^{2+} (Eliasson et al., 1996). We therefore examined the effect of glucose on endocytosis in cell-attached membrane patches of INS-1 cells. Upon bath perfusion of 10 mM glucose, which maximally stimulates insulin secretion (Hohmeier and Newgard, 2004), 430 endocytotic events were observed in membrane patches from 48 cells. The rate of membrane

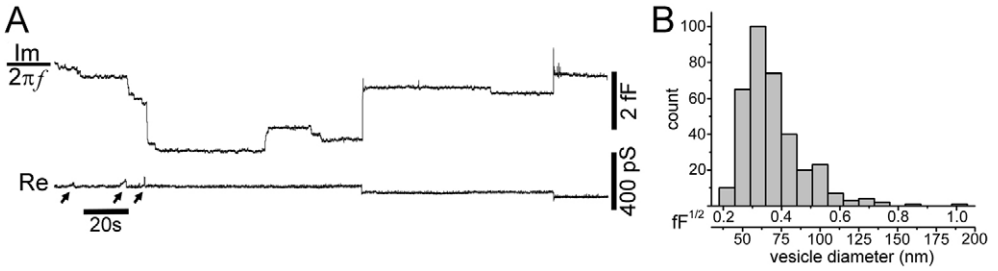

Fig. 1. Endocytosis of single vesicles in INS-1 β-cells. (A) A cell-attached recording where step-wise changes in capacitance (Im/2π*f*) represent exocytosis (upward) and endocytosis (downward) of single vesicles. Transient changes in conductance (Re) during a capacitance step (arrows) result from the formation of fission pores. Step-wise changes in Re upon a capacitance step result from small phase offsets, which were corrected off-line prior to further analysis. (B) The size distribution, shown both as the square root of capacitance ($fF^{1/2}$) and vesicle diameter, of endocytotic events observed in cell-attached recordings with 2.6 mM Ca^{2+} in the patch-pipette and 0 mM glucose/0 mM Ca^{2+} in the bath.

internalisation upon glucose stimulation was increased to 8.5±1.1 μm^2 $cell^{-1}$ $minute^{-1}$ (P<0.05; Fig. 2A). Surprisingly, this was not owing to an increased frequency of endocytosis (2.2±0.3 $patch^{-1}$ $minute^{-1}$, not significant; Fig. 2B), but rather was largely the result of an increase in average endocytotic vesicle capacitance to 240±17 aF (P<0.001; Fig. 2C).

We next examined whether Ca^{2+} entry was responsible for the glucose-induced increase in endocytotic vesicle size. In all cell-attached experiments, Ca^{2+} was absent from the bath to ensure Ca^{2+} entry only through channels within the membrane patch directly beneath the Ca^{2+}-containing pipette. We observed 512 endocytotic events in 52 membrane patches in the complete absence of Ca^{2+}, and 340 events in 50 patches with 10 mM Ca^{2+} in the patch-pipette. Glucose (10 mM) was present in the bath for these experiments. Varying pipette-Ca^{2+} did not alter the frequency of endocytotic events (Fig. 3A). When Ca^{2+} was absent from the patch-pipette, endocytotic vesicle capacitance was decreased compared with 2.6 mM Ca^{2+} (171±7 aF, P<0.001; Fig. 3B). The effect of Ca^{2+} was bimodal, and with a pipette-Ca^{2+} concentration of 10 mM, vesicle capacitance was 201±19 aF (Fig. 3B).

L- and R-type Ca^{2+} channels are important mediators of insulin secretion (Jing et al., 2005; Rorsman and Renstrom, 2003). In the presence of the L-type Ca^{2+} channel inhibitor isradipine (2 μM), 399 endocytotic events were observed in 50 membrane patches. When the R-type Ca^{2+} channel inhibitor SNX-482 was present (100 nM), 411 endocytotic events were observed in 42 patches. Both of these inhibitors prevented the Ca^{2+}-induced increase in endocytotic vesicle capacitance (Fig. 3C), but had no significant effect on endocytotic event frequency (isradipine: 1.7±0.3 $patch^{-1}$ $minute^{-1}$; SNX-482: 2.5±0.3 $patch^{-1}$ $minute^{-1}$).

Endocytosis in cell-free excised membrane patches

The direct effect of Ca^{2+} on endocytotic vesicle size was investigated further by application of Ca^{2+} to the intracellular surface of inside-out excised membrane patches. Experiments were performed in the absence of Ca^{2+} and presence of 2 mM EGTA, where 136 endocytotic events were observed in 18 excised membrane patches; with 100 nM free-Ca^{2+}, where 102 events were detected in 19 patches; and with 0.5 mM Ca^{2+}, where 114 events were observed in 16 patches. In these experiments, 100 nM free-Ca^{2+} stimulated a 3.6-fold increase in the frequency of exocytotic events (not shown). By contrast, the endocytotic event frequency was not significantly increased with 100 nM free-Ca^{2+} or 0.5 mM Ca^{2+} compared with the unstimulated condition (Fig. 4A). The size distribution of

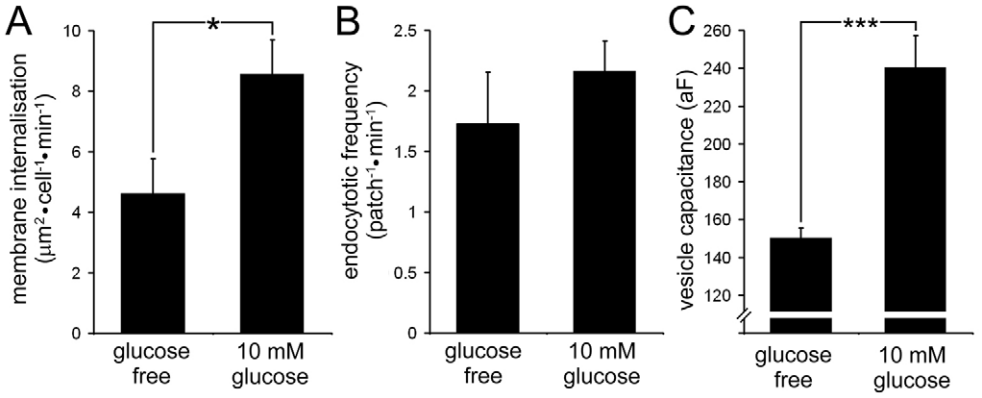

Fig. 2. Glucose stimulation enhances membrane internalisation and increases endocytotic vesicle size in INS-1 cells. Experiments were performed with 2.6 mM Ca^{2+} in the patch-pipette and 0 mM Ca^{2+} in the bath. (A) The rate of membrane internalisation is increased when 10 mM glucose is present in the bath. (B) Glucose did not increase the frequency at which endocytotic events occurred. (C) Glucose increased the unitary capacitance of endocytotic steps, reflecting a significant increase in endocytotic vesicle size. *, P<0.05; ***, P<0.001.

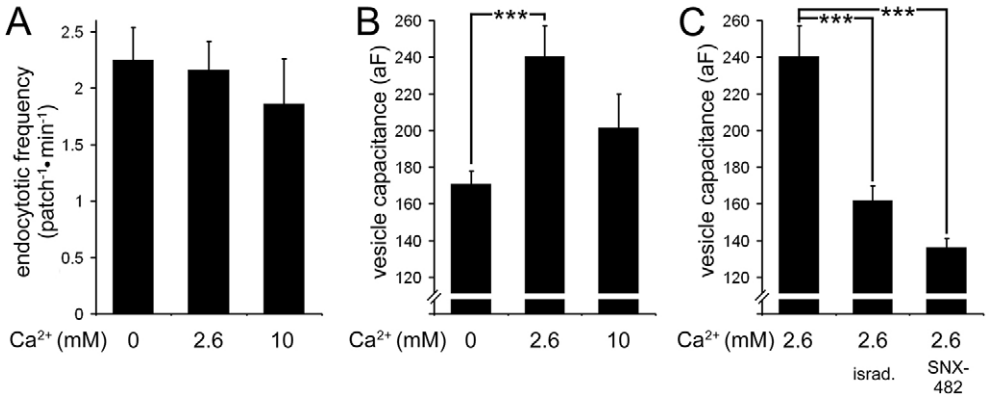

Fig. 3. Endocytotic vesicle size is regulated in a bimodal manner by Ca^{2+} entry through voltage-dependent channels in INS-1 cells. Experiments were performed with 10 mM glucose and 0 mM Ca^{2+} in the bath, and pipette-Ca^{2+} was varied. (A) The frequency of endocytotic events was unchanged at different pipette-Ca^{2+} concentrations. (B) Inclusion of 2.6 mM Ca^{2+} in the patch-pipette significantly increased the unitary capacitance of endocytotic steps, indicating an increase in vesicle size. This effect was ameliorated by further increasing pipette-Ca^{2+} to 10 mM. (C) With 2.6 mM Ca^{2+} in the patch-pipette, inclusion of the L-type Ca^{2+} channel inhibitor isradipine (israd., 2 μM) or the R-type Ca^{2+} channel inhibitor SNX-482 (100 nM) prevented the Ca^{2+}-dependent increase in endocytotic vesicle capacitance. ***, $P<0.001$.

endocytotic events observed in the absence of Ca^{2+} stimulation is shown in Fig. 4B. Similar to a previous report (Dernick et al., 2003), endocytotic vesicles observed in excised patches in the absence of Ca^{2+} were significantly ($P<0.001$) larger, at 226±14 aF, than those in cell-attached patches. Stimulation with 100 nM free-Ca^{2+} increased endocytotic vesicle capacitance further to 299±26 aF ($P<0.001$) and, in agreement with observations in the cell-attached experiments, the effect of Ca^{2+} was bimodal and 0.5 mM Ca^{2+} did not increase vesicle size (Fig. 4C).

Analysis of endocytotic fission pore conductance

Transient increases in patch conductance (Re) immediately preceding an endocytotic event, such as those observed in Fig. 1B (arrows), reflect the detection of a fission pore (Rosenboom and Lindau, 1994). The endocytotic event in Fig. 5 is shown following off-line phase correction (see Materials and Methods). The imaginary (Im) conductance component reflects patch capacitance whereas the real (Re) component reflects patch conductance. The true vesicle capacitance, C_v, and pore conductance, G_p, are calculated from Re and Im (Lollike and Lindau, 1999) and are shown in the right panels of Fig. 5. Twenty-nine endocytotic fission pores were examined initially. As observed at the arrow marked (i), the fission pore is first detected as G_p decreases to a measurable level. From here, pore conductance decreased with a time constant (τ) of 284±30 ms, resulting from pore lengthening and/or constriction (marked ii). Finally, pore conductance abruptly decreases (at the arrow marked iii), representing closure of the fission pore and removal of the endocytotic vesicle from the patch membrane as indicated by the simultaneous decrease in C_v. On average, the final G_p prior to fission pore closure was 118±24 pico-Siemen (pS).

Calcium entry regulates fission pore kinetics

We examined the kinetics of a further 180 endocytotic fission pores detected in the cell-attached patch experiments. Glucose stimulation significantly accelerated the decay time constant of

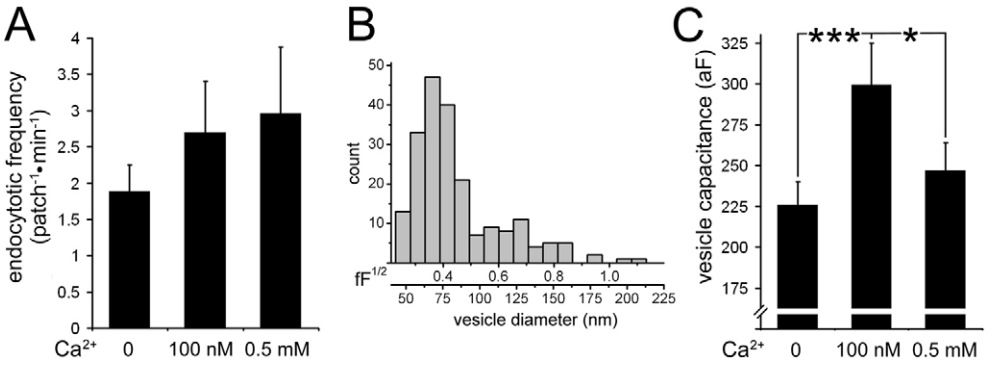

Fig. 4. Endocytotic vesicle capacitance is regulated by direct application of Ca^{2+} to inside-out excised membrane patches from INS-1 cells. (A) The frequency of endocytotic events in the excised patch was not changed significantly by bath application of Ca^{2+} (100 nM free, or 0.5 mM). (B) The size distribution, both as the square root of capacitance ($fF^{1/2}$) and vesicle diameter, of endocytotic events observed in excised-patch recordings in the absence of Ca^{2+}. (C) Bath application of a buffered 100 nM free-Ca^{2+} solution increased vesicle capacitance. Similar to the cell-attached experiments, this effect was bimodal, and did not occur upon application of 0.5 mM Ca^{2+}. *, $P<0.05$; ***, $P<0.001$.

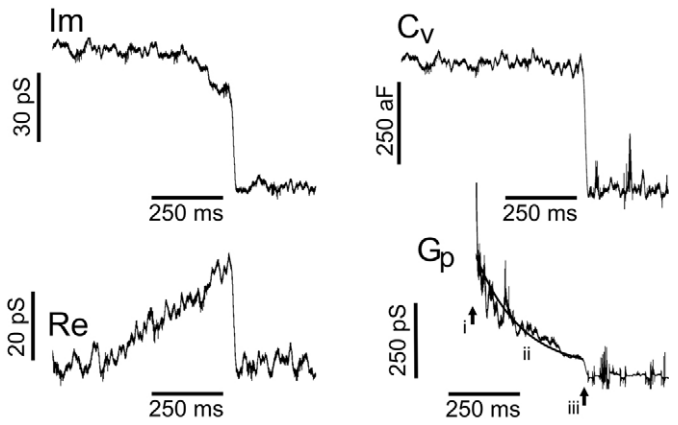

Fig. 5. Analysis of endocytotic fission pore kinetics. In the left panels, the imaginary (Im) conductance component reflects membrane patch capacitance, whereas the real (Re) component reflects the patch conductance. A transient increase in Re immediately prior to endocytosis reflects the endocytotic fission pore. In the right panels, the endocytotic vesicle capacitance (C_v) and fission pore conductance (G_p) were calculated from Im and Re (see Materials and Methods). After formation, the reduction of fission pore conductance reflects either the constriction or lengthening of the pore. The kinetics of this was examined by fitting G_p with a single exponential decay function (solid line). As observed at the arrow marked (i), the fission pore is first detected as G_p decreases to a measurable level. From here, pore conductance decays (marked ii) and finally decreases abruptly to zero (at the arrow marked iii), representing closure of the fission pore and removal of the endocytotic vesicle from the patch membrane as indicated by the simultaneous decrease in C_v.

fission pore conductance to 216±21 ms (N=30, P<0.05). This effect was prevented by removal of Ca^{2+} from the patch-pipette (N=26; Fig. 6A,B), suggesting a dependence on Ca^{2+} influx. Indeed, the effect of Ca^{2+} removal was mimicked by including 2 μM isradipine (N=41) or 100 nM SNX-482 (N=26) in the patch-pipette (Fig. 6C,D). With 10 mM Ca^{2+} in the pipette, the rate at which pore conductance decreased was accelerated (τ=220±20, N=57, P<0.05) compared with that in the absence of Ca^{2+}, but was not different from that seen at 2.6 mM Ca^{2+}. The average conductance measured prior to fission pore closure under glucose-stimulated conditions was 141±27 pS (N=31), which was no different from that observed in the absence of glucose, and was unaffected by the other conditions (not shown).

In the inside-out excised membrane patches, 52 fission pores were examined. Pore conductance decreased with a time constant (τ) of 580±113 ms (N=15) in the absence of Ca^{2+} stimulation (Fig. 7), which is significantly slower than the rate observed in the unstimulated condition in cell-attached experiments (P<0.05). We considered whether this was secondary to the increased endocytotic vesicle size in excised patches; however, the fission time constant was not correlated to vesicle capacitance within either the cell-attached (R^2=2.4×10^{-3}, P>0.45) or excised-patch experiments (R^2=1.7×10^{-4}, P>0.90). The rate of fission was increased (τ=275±45 ms, N=21, P>0.05) in the presence of 100 nM free-Ca^{2+} (Fig. 7). Increasing Ca^{2+} to 0.5 mM did not further quicken the rate of fission (τ=189±33 ms, N=16).

Calcineurin regulates endocytotic frequency and vesicle size, but not fission kinetics

Calcineurin is probably an important mediator of Ca^{2+} effects on endocytosis since it mediates the Ca^{2+}-dependent dephosphorylation of numerous endocytotic proteins (Cousin and Robinson, 2001). We therefore applied to

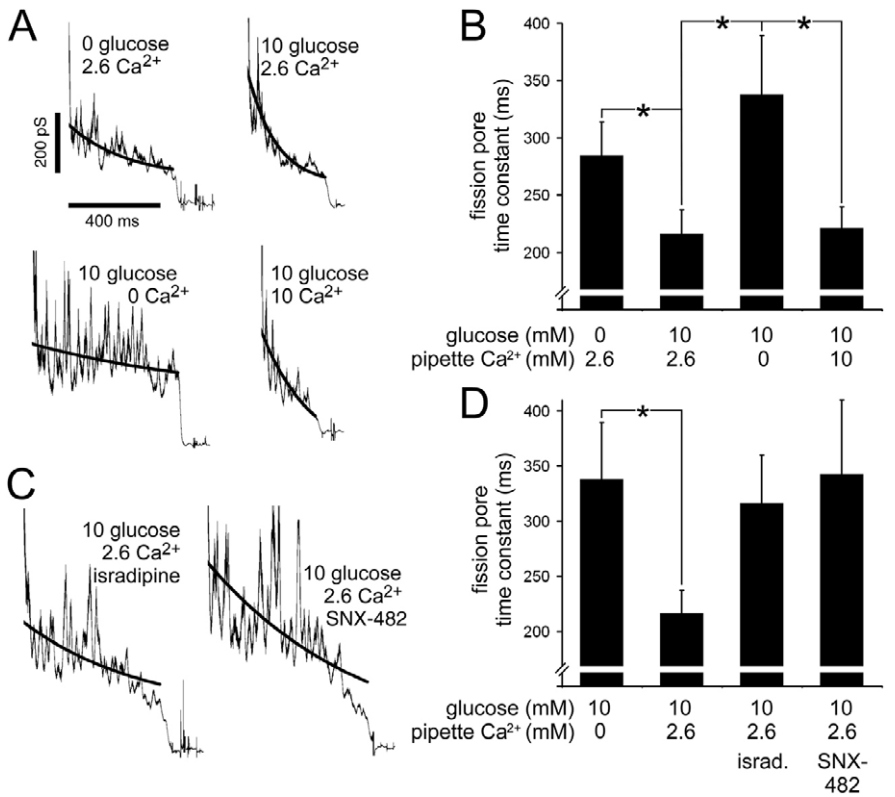

Fig. 6. Acceleration of membrane fission kinetics by glucose-dependent Ca^{2+} entry in INS-1 cells. Experiments were performed in the cell-attached configuration. In the bath, Ca^{2+} was absent and glucose was varied between 0 and 10 mM. In the patch-pipette, Ca^{2+} was varied and channel inhibitors were included as indicated. Changes in fission pore conductance (G_p) were fit with single exponential decay functions. (A,B) With 2.6 mM Ca^{2+} in the patch-pipette, glucose stimulation accelerated the kinetics of membrane fission, indicated by a more rapid decrease in fission pore conductance and a faster fission pore time constant (τ). This glucose-dependent acceleration was prevented by removal of Ca^{2+} from the patch-pipette, but was not further increased when 10 mM Ca^{2+} was present. (C,D) In the presence of 10 mM glucose, the acceleration of membrane fission observed with 2.6 mM Ca^{2+} present in the patch-pipette was prevented by inclusion of the L-type Ca^{2+} channel inhibitor isradipine (2 μM) or the R-type Ca^{2+} channel inhibitor SNX-482 (100 nM). *, P<0.05.

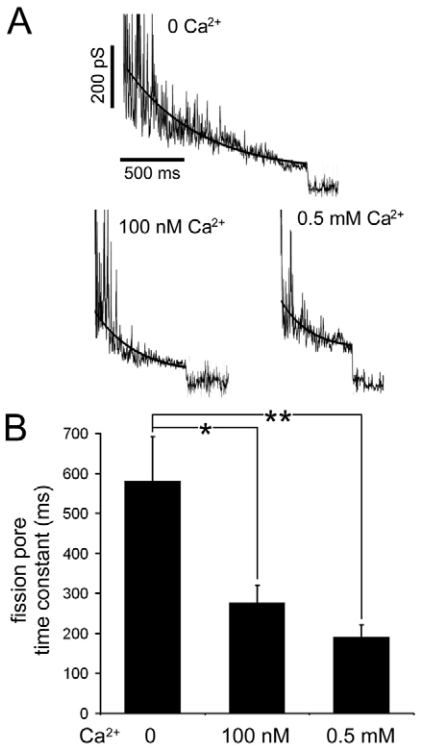

Fig. 7. Acceleration of membrane fission by Ca^{2+} in inside-out excised membrane patches from INS-1 cells. Changes in fission pore conductance (G_p) were fit with single exponential decay functions. Bath application of a 100 nM free-Ca^{2+} buffer or 0.5 mM Ca^{2+} accelerated the kinetics of membrane fission. (A) Representative G_p traces with 0 mM Ca^{2+}, 100 nM free-Ca^{2+} or 0.5 mM Ca^{2+} in the bath. (B) Fission pore time constants (τ) were calculated by fitting the G_p traces with single exponential decay functions. Unlike what was seen with endocytotic vesicle size, the effect of Ca^{2+} on fission kinetics was not bimodal. *, $P<0.05$; **, $P<0.01$.

the intracellular surface of excised patches either the calcineurin inhibitor deltamethrin (1 μM) or purified calcineurin (0.4 U/ml). With deltamethrin, 106 events were observed in 16 excised patches. With calcineurin, excess calmodulin (100 U/ml) was also included as this is necessary for calcineurin activation, and 170 events were detected in 13 excised patches. Exogenous calcineurin/calmodulin increased endocytotic frequency to 5.2±1.2 patch^{-1} minute^{-1} ($P<0.05$), whereas the calcineurin inhibitor deltamethrin was without effect in this respect (Fig. 8A). This suggests that whereas calcineurin is not an endogenous regulator of endocytotic frequency in INS-1 cells, it might increase the occurrence of endocytotic events when present at sufficient levels. However, deltamethrin prevented the Ca^{2+}-induced increase in endocytotic vesicle capacitance, whereas exogenous calcineurin did not significantly affect vesicle size (Fig. 8B). Thus, although the Ca^{2+}-dependent activation of endogenous calcineurin is sufficient to increase vesicle size, exogenous calcineurin has no further effect. Neither deltamethrin nor calcineurin/calmodulin treatment significantly altered fission kinetics (Fig. 8C), suggesting an alternate Ca^{2+} sensor. This is surprising given the known importance of Ca^{2+}/calcineurin-dependent dephosphorylation of dynamin (Smillie and Cousin, 2005).

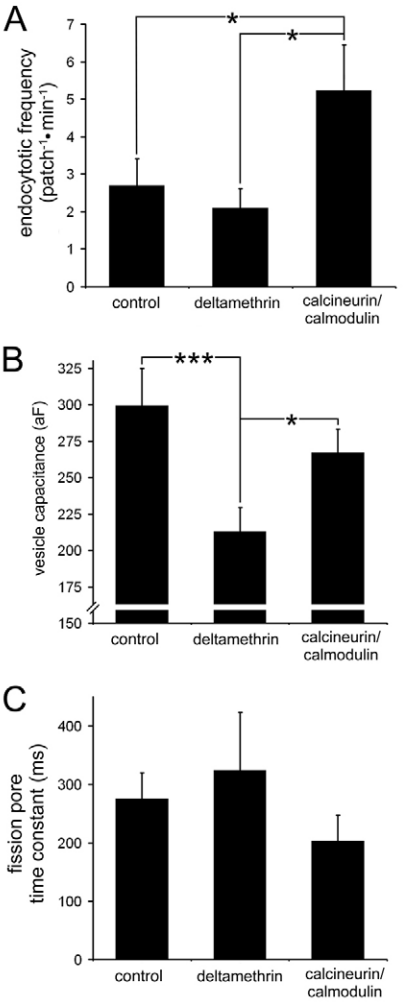

Fig. 8. The Ca^{2+}-dependent increase in endocytotic vesicle size, but not the Ca^{2+}-dependent acceleration of fission kinetics, is prevented by inhibition of calcineurin. Experiments were performed on inside-out excised membrane patches from INS-1 cells in the presence of a 100 nM free-Ca^{2+} buffer. (A) The frequency at which endocytotic events occurred was not changed by the calcineurin inhibitor deltamethrin (1 μM), but was increased in the presence of exogenous purified calcineurin (0.4 U/ml) and calmodulin (100 U/ml). (B) Antagonism of calcineurin with deltamethrin prevented the Ca^{2+}-induced increase in endocytotic vesicle capacitance, whereas exogenous calcineurin/calmodulin had no effect. The control condition in this case represents vesicle capacitance during 100 nM free-Ca^{2+} stimulation. (C) Neither antagonism of calcineurin with deltamethrin nor exogenous calcineurin/calmodulin significantly affected the rate of membrane fission during 100 nM free-Ca^{2+} stimulation. *, $P<0.05$; ***, $P<0.001$.

Discussion

In many cells, the Ca^{2+}-dependent upregulation of endocytosis is likely to couple membrane retrieval to exocytosis. The phosphatase calcineurin is a potential Ca^{2+} sensor for this (Jarousse and Kelly, 2001; Murthy and De Camilli, 2003; Wu, 2004), however no study has characterised Ca^{2+} effects on endocytosis and membrane fission at the single-vesicle level. Here we consider, using (neuro)endocrine INS-1 cells as a

model system: (1) the effects of glucose and Ca^{2+} on membrane retrieval and endocytotic vesicle size; (2) the regulation of endocytotic fission pore kinetics; and (3) the potential role of calcineurin in the observed Ca^{2+}-dependent effects.

Glucose and calcium effects on membrane retrieval and endocytotic vesicle size

The ability of glucose to enhance endocytotic membrane retrieval reported here is not without precedent in β-cells as horseradish peroxidase uptake is reported to be increased by glucose (Orci et al., 1973). Moreover, endocytosis in these cells, which occurs with a slower time course than exocytosis (Ammala et al., 1993), is accelerated by Ca^{2+} (Eliasson et al., 1996). It was however surprising that endocytotic frequency was not significantly changed by glucose or Ca^{2+}. By far the most pronounced effect was on vesicle capacitance, indicating a glucose- and Ca^{2+}-dependent increase in vesicle size. In β-cells, Ca^{2+} entry through L-type channels triggers exocytosis of the readily releasable vesicle pool (Rorsman and Renstrom, 2003), following which Ca^{2+} influx through R-type channels mediates continued insulin release (Jing et al., 2005). In sea urchin eggs, insertion of P-type Ca^{2+} channels into the plasma membrane by stimulated exocytosis is essential for compensatory endocytosis (Smith et al., 2000; Vogel et al., 1999), and a similar hierarchical role for L-type and R-type channels in the INS-1 cells could explain the ability of either L- or R-type channel inhibitors to prevent the glucose effects on vesicle size and fission kinetics.

Few studies have addressed the regulation of endocytotic vesicle size. Actin cytoskeleton disruption in rat melanotrophs reduced the size of endocytotic vesicles (Chowdhury et al., 2002) and excision of membrane patches from rat chromaffin cells increased vesicle size (Dernick et al., 2003). The latter observation is confirmed in the INS-1 cells where endocytotic vesicles observed in excised membrane patches were 50% larger than those observed in intact cells (Fig. 5). These data indicate an important role for cytoskeletal elements in the regulation of vesicle size. Indeed, the adaptor protein eps15, a regulator of endocytosis (Carbone et al., 1997; Wendland et al., 1996), mediates an indirect interaction between the actin cytoskeleton and proteins involved in clathrin assembly, including AP180 (Duncan et al., 2001; Wendland and Emr, 1998). Mutation of AP180 homologues in *Caenorhabditis elegans* and *Drosophila* increased synaptic vesicle size as a result of altered vesicle biogenesis at the point of endocytosis (Nonet et al., 1999; Zhang et al., 1998), and AP180 regulates the size of clathrin cages in vitro (Ye and Lafer, 1995). Interestingly, AP180 is one of a number of endocytotic proteins that are regulated in a Ca^{2+}-dependent manner by the phosphatase calcineurin (Cousin and Robinson, 2001).

Glucose and calcium effects on the kinetics of membrane fission

Conventional endocytosis is characterised by recruitment of coat proteins, vesicle budding and dynamin-mediated closure of the membrane fission pore (Jarousse and Kelly, 2001). The late stages of this process, seen as changes in fission pore conductance, have been examined previously during the internalisation of large 100-200 fF (2-3 μm diameter) vacuoles (Eliasson et al., 1996; Rosenboom and Lindau, 1994; Suss-Toby et al., 1996). Although one recent study reports the detection of a fission pore during endocytosis of a 3 fF (325 nm diameter) vesicle in chromaffin cells (Dernick et al., 2003), we have for the first time characterised the fission kinetics of very small endocytotic vesicles similar in size to synaptic vesicles, ranging from 107 aF to 1.3 fF (62-214 nm diameter). These small vesicles are likely to be responsible for the majority of endocytotic activity in cells. Fission pores were detected during 10% of the endocytotic events, and we found that larger vesicles were more often associated with a detectable fission pore. However, since this is similar to the detection rate reported previously during step-wise exocytosis of small vesicles (Klyachko and Jackson, 2002), and we found no correlation between vesicle size and fission kinetics, we believe that our results are indeed representative.

In two studies (Rosenboom and Lindau, 1994; Suss-Toby et al., 1996), fission pores were characterised by intermediate semi-stable conductance phases and a slow conductance decrease to zero, indicating pore constriction and closure. The data presented here agree with the presence of a semi-stable fission pore that decreases in conductance with a relatively slow time constant. However, similar to what was observed for endocytosis of large vacuoles, or possibly multi-granule complexes, in β-cells (Eliasson et al., 1996) and during endocytosis in excised patches of chromaffin cells (Dernick et al., 2003), we find that once pore conductance reached a certain point, final closure of the fission pore nearly always occurred abruptly. The conductance from which pore closure occurred was constant and unaffected by different treatments, indicating a tightly controlled mechanism catalysing final membrane fission once pore conductance reaches a crucial point.

After fission pore formation, G_p decreases as a result of either constriction or lengthening of the pore and the present data cannot differentiate between the two possibilities. We have however demonstrated that glucose-dependent Ca^{2+} entry through voltage-dependent channels in intact cells, and direct Ca^{2+} application to isolated membrane patches, increases the rate of membrane fission. This is strikingly similar to the ability of Ca^{2+} to enhance the rate of exocytotic fusion pore expansion (Fernandez-Chacon and Alvarez, 1995; Haller et al., 2001; Hartmann and Lindau, 1995; Scepek et al., 1998), perhaps suggesting a similar mechanism controlling fission pore constriction and fusion pore expansion. One interesting possibility is a Ca^{2+}-dependent increase in membrane and/or cytoskeleton rigidity (Liu et al., 2005; Shields et al., 1987), which might be expected to increase the elastic energy of membrane vesicles and intermediate membrane structures mediating pore closing or opening. However, it does not appear that the Ca^{2+} effect on fission involves calcineurin, since neither exogenous calcineurin nor its inhibitor deltamethrin altered pore kinetics.

Calcineurin as a potential mediator of the calcium effects

Much work remains to determine the mechanism of the observed Ca^{2+}-dependent increase in endocytotic vesicle size and acceleration of fission pore kinetics. In endocrine chromaffin cells, endocytosis is dependent on Ca^{2+} and calmodulin (Artalejo et al., 1995; Artalejo et al., 1996),

although there appear to be distinct calcineurin-dependent and -independent pathways (Chan and Smith, 2001; Engisch and Nowycky, 1998). Also, calcineurin has been implicated previously in the regulation of inositol hexakisphosphate-stimulated endocytosis in β-cells (Hoy et al., 2002b). We have thus begun to examine a role for the phosphatase calcineurin, which is activated by a Ca^{2+}-dependent interaction with calmodulin (Klee et al., 1979; Yang et al., 1982) and catalyses the dephosphorylation of numerous proteins involved in endocytosis (Cousin and Robinson, 2001). Consistent with its role as a positive regulator of endocytosis, excess calcineurin enhanced endocytotic frequency. The physiological relevance of this is not clear in INS-1 cells since no other treatment altered endocytotic frequency, including the physiological stimulus glucose. Alternatively, as calmodulin was also included in those experiments, it is possible that increased endocytotic frequency results from the activation of alternate effectors such as myosin light chain kinase or the calcium/calmodulin-dependent kinase (CaMK) enzymes (Nairn and Picciotto, 1994).

On the basis of the effects of the calcineurin inhibitor deltamethrin, endogenous calcineurin activity is implicated in the ability of Ca^{2+} to increase endocytotic vesicle size but not in Ca^{2+}-dependent acceleration of membrane fission. A role for separate Ca^{2+} sensors for these effects is supported by their differential responses to high Ca^{2+} levels. Numerous endocytotic proteins involved in clathrin coat assembly and/or interaction with the cytoskeleton, including AP180, epsin and eps15, are dephosphorylated by calcineurin and collectively referred to as the dephosphins (Cousin and Robinson, 2001). The mechanism by which regulation of the dephosphins might modulate endocytotic vesicle size is unclear, however, as further information is needed about how the phosphorylation status of these proteins regulates their function and protein-protein interactions.

Inhibition of endocytosis by high Ca^{2+} levels has been reported previously (Rouze and Schwartz, 1998; von Gersdorff and Matthews, 1994b) and reducing Ca^{2+} at the active zone by inhibiting Ca^{2+} channels or chelating Ca^{2+} relieves a tonic inhibition of endocytosis (Cousin and Robinson, 2000). The mechanism for inhibition of endocytosis induced by high Ca^{2+} levels might involve a direct inhibitory effect on dynamin GTPase activity (Cousin and Robinson, 2000) or perhaps the synaptotagmin-dependent sequesteration of phosphatidylinositol (4,5)-bisphosphate, which is necessary for dynamin-dependent endocytosis, when Ca^{2+} levels are high (Cousin, 2000; Schiavo et al., 1996). However, it seems unlikely that inhibition of dynamin is responsible for the bimodal response of endocytotic vesicle size to Ca^{2+} observed in the present study since we observed no bimodal effect on the rate of fission, in which dynamin is expected to play a central role.

Conclusions

Ca^{2+}-dependent regulation of endocytotic vesicle size and membrane fission compensates, at least in part, for membrane added by the stimulated exocytosis of insulin-containing dense-core vesicles and gamma-aminobutryic acid (GABA)-containing synaptic-like vesicles. Rapid endocytosis characterised by whole-cell capacitance measurements correlates with the retrieval of intact vesicles by a 'kiss-and-run' mechanism (Neher and Zucker, 1993; Thomas et al., 1994; von Gersdorff and Matthews, 1994a). Current evidence suggests that 'kiss-and-run' contributes to only a minor fraction of the recycling of dense-core vesicles in these cells (Ma et al., 2004; MacDonald et al., 2005; Takahashi et al., 2002). The events characterised in the present study did not follow previous exocytosis and are therefore likely to represent the de novo formation of endocytotic vesicles rather than 'kiss-and-run'. Accordingly, we conclude that the majority of dense-core vesicle membranes in these cells are retrieved by the upregulation of conventional endocytosis, and in particular an increase in endocytotic vesicle size. We have here identified a Ca^{2+}-dependent increase in endocytotic vesicle size and acceleration of membrane fission as a novel mechanism mediating the stimulation-dependent upregulation of endocytosis in insulin-secreting cells.

Studies in Sweden were supported by the Novo Nordisk Foundation, the Swedish Strategic Foundation, the Goran Gustafsson Foundation for Research in the Natural Sciences and Medicine, the Swedish Research Council (13147; L.E.), and the Faculty of Medicine, Lund University. Work in the UK was supported by the Wellcome Trust. P.E.M. was initially supported by a Canadian Institutes of Health Research Fellowship and currently by the European Foundation for the Study of Diabetes/AstraZeneca Fellowship in Islet Biology. P.R. is a Royal Society-Wolfson Research Fellow.

References

Albillos, A., Dernick, G., Horstmann, H., Almers, W., Alvarez de Toledo, G. and Lindau, M. (1997). The exocytotic event in chromaffin cells revealed by patch amperometry. *Nature* **389**, 509-512.

Ammala, C., Eliasson, L., Bokvist, K., Larsson, O., Ashcroft, F. M. and Rorsman, P. (1993). Exocytosis elicited by action potentials and voltage-clamp calcium currents in individual mouse pancreatic. B-cells *J. Physiol.* **472**, 665-688.

Artalejo, C. R., Henley, J. R., McNiven, M. A. and Palfrey, H. C. (1995). Rapid endocytosis coupled to exocytosis in adrenal chromaffin cells involves Ca^{2+}, GTP, and dynamin but not clathrin. *Proc. Natl. Acad. Sci. USA* **92**, 8328-8332.

Artalejo, C. R., Elhamdani, A. and Palfrey, H. C. (1996). Calmodulin is the divalent cation receptor for rapid endocytosis, but not exocytosis, in adrenal chromaffin cells. *Neuron* **16**, 195-205.

Bauerfeind, R., Takei, K. and De Camilli, P. (1997). Amphiphysin I is associated with coated endocytic intermediates and undergoes stimulation-dependent dephosphorylation in nerve terminals. *J. Biol. Chem.* **272**, 30984-30992.

Carbone, R., Fre, S., Iannolo, G., Belleudi, F., Mancini, P., Pelicci, P. G., Torrisi, M. R. and Di Fiore, P. P. (1997). eps15 and eps15R are essential components of the endocytic pathway. *Cancer Res.* **57**, 5498-5504.

Chan, S. A. and Smith, C. (2001). Physiological stimuli evoke two forms of endocytosis in bovine chromaffin cells. *J. Physiol.* **537**, 871-885.

Chowdhury, H. H., Kreft, M. and Zorec, R. (2002). Distinct effect of actin cytoskeleton disassembly on exo- and endocytic events in a membrane patch of rat melanotrophs. *J. Physiol.* **545**, 879-886.

Cousin, M. A. (2000). Synaptic vesicle endocytosis: calcium works overtime in the nerve terminal. *Mol. Neurobiol.* **22**, 115-128.

Cousin, M. A. and Robinson, P. J. (2000). Ca^{2+} influx inhibits dynamin and arrests synaptic vesicle endocytosis at the active zone. *J. Neurosci.* **20**, 949-957.

Cousin, M. A. and Robinson, P. J. (2001). The dephosphins: dephosphorylation by calcineurin triggers synaptic vesicle endocytosis. *Trends Neurosci.* **24**, 659-665.

Debus, K. and Lindau, M. (2000). Resolution of patch capacitance recordings and of fusion pore conductances in small vesicles. *Biophys. J.* **78**, 2983-2997.

Dernick, G., Alvarez, d. T. and Lindau, M. (2003). Exocytosis of single chromaffin granules in cell-free inside-out membrane patches. *Nat. Cell Biol.* **5**, 358-362.

Duncan, M. C., Cope, M. J., Goode, B. L., Wendland, B. and Drubin, D. G. (2001). Yeast Eps15-like endocytic protein, Pan1p, activates the Arp2/3 complex. *Nat. Cell Biol.* **3**, 687-690.

Eliasson, L., Proks, P., Ammala, C., Ashcroft, F. M., Bokvist, K., Renstrom, E., Rorsman, P. and Smith, P. A. (1996). Endocytosis of secretory granules in mouse pancreatic beta-cells evoked by transient elevation of cytosolic calcium. *J. Physiol.* **493**, 755-767.

Engisch, K. L. and Nowycky, M. C. (1998). Compensatory and excess retrieval: two types of endocytosis following single step depolarizations in bovine adrenal chromaffin cells. *J. Physiol.* **506**, 591-608.

Fernandez-Chacon, R. and Alvarez, d. T. (1995). Cytosolic calcium facilitates release of secretory products after exocytotic vesicle fusion. *FEBS Lett.* **363**, 221-225.

Haller, T., Dietl, P., Pfaller, K., Frick, M., Mair, N., Paulmichl, M., Hess, M. W., Furst, J. and Maly, K. (2001). Fusion pore expansion is a slow, discontinuous, and Ca^{2+}-dependent process regulating secretion from alveolar type II cells. *J. Cell Biol.* **155**, 279-289.

Hartmann, J. and Lindau, M. (1995). A novel Ca^{2+}-dependent step in exocytosis subsequent to vesicle fusion. *FEBS Lett.* **363**, 217-220.

Henkel, A. W., Horstmann, H. and Henkel, M. K. (2001). Direct observation of membrane retrieval in chromaffin cells by capacitance measurements. *FEBS Lett.* **505**, 414-418.

Hohmeier, H. E. and Newgard, C. B. (2004). Cell lines derived from pancreatic islets. *Mol. Cell Endocrinol.* **228**, 121-128.

Hoy, M., Efanov, A. M., Bertorello, A. M., Zaitsev, S. V., Olsen, H. L., Bokvist, K., Leibiger, B., Leibiger, I. B., Zwiller, J., Berggren, P. O. et al. (2002a). Inositol hexakisphosphate promotes dynamin I- mediated endocytosis. *Proc. Natl. Acad. Sci. USA* **99**, 6773-6777.

Hoy, M., Efanov, A. M., Bertorello, A. M., Zaitsev, S. V., Olsen, H. L., Bokvist, K., Leibiger, B., Leibiger, I. B., Zwiller, J., Berggren, P. O. et al. (2002b). Inositol hexakisphosphate promotes dynamin I-mediated endocytosis. *Proc. Natl. Acad. Sci. USA* **99**, 6773-6777.

Jarousse, N. and Kelly, R. B. (2001). Endocytotic mechanisms in synapses. *Curr. Opin. Cell Biol.* **13**, 461-469.

Jing, X., Li, D. Q., Olofsson, C. S., Salehi, A., Surve, V. V., Caballero, J., Ivarsson, R., Lundquist, I., Pereverzev, A., Schneider, T. et al. (2005). Cav2.3 calcium channels control second-phase insulin release. *J. Clin. Invest* **115**, 146-154.

Klee, C. B., Crouch, T. H. and Krinks, M. H. (1979). Calcineurin: a calcium- and calmodulin-binding protein of the nervous system. *Proc. Natl. Acad. Sci. USA* **76**, 6270-6273.

Klyachko, V. A. and Jackson, M. B. (2002). Capacitance steps and fusion pores of small and large-dense-core vesicles in nerve terminals. *Nature* **418**, 89-92.

Kreft, M. and Zorec, R. (1997). Cell-attached measurements of attofarad capacitance steps in rat melanotrophs. *Pflugers Arch.* **434**, 212-214.

Liu, F., Mizukami, H., Sarnaik, S. and Ostafin, A. (2005). Calcium-dependent human erythrocyte cytoskeleton stability analysis through atomic force microscopy. *J. Struct. Biol.* **150**, 200-210.

Liu, J. P., Sim, A. T. and Robinson, P. J. (1994). Calcineurin inhibition of dynamin I GTPase activity coupled to nerve terminal depolarization. *Science* **265**, 970-973.

Lollike, K. and Lindau, M. (1999). Membrane capacitance techniques to monitor granule exocytosis in neutrophils. *J. Immunol. Methods* **232**, 111-120.

Lollike, K., Borregaard, N. and Lindau, M. (1995). The exocytotic fusion pore of small granules has a conductance similar to an ion channel. *J. Cell Biol.* **129**, 99-104.

Ma, L., Bindokas, V. P., Kuznetsov, A., Rhodes, C., Hays, L., Edwardson, J. M., Ueda, K., Steiner, D. F. and Philipson, L. H. (2004). Direct imaging shows that insulin granule exocytosis occurs by complete vesicle fusion. *Proc. Natl. Acad. Sci. USA* **101**, 9266-9271.

MacDonald, P. E., Obermuller, S., Vikman, J., Galvanovskis, J., Rorsman, P. and Eliasson, L. (2005). Regulated exocytosis and kiss-and-run of synaptic-like microvesicles in INS-1 and primary rat beta-cells. *Diabetes* **54**, 736-743.

Marks, B. and McMahon, H. T. (1998). Calcium triggers calcineurin-dependent synaptic vesicle recycling in mammalian nerve terminals. *Curr. Biol.* **8**, 740-749.

Murthy, V. N. and De Camilli, P. (2003). Cell biology of the presynaptic terminal. *Annu. Rev. Neurosci.* **26**, 701-728.

Nairn, A. C. and Picciotto, M. R. (1994). Calcium/calmodulin-dependent protein kinases. *Semin. Cancer Biol.* **5**, 295-303.

Neher, E. and Marty, A. (1982). Discrete changes of cell membrane capacitance observed under conditions of enhanced secretion in bovine adrenal chromaffin cells. *Proc. Natl. Acad. Sci. USA* **79**, 6712-6716.

Neher, E. and Zucker, R. S. (1993). Multiple calcium-dependent processes related to secretion in bovine chromaffin cells. *Neuron* **10**, 21-30.

Nonet, M. L., Holgado, A. M., Brewer, F., Serpe, C. J., Norbeck, B. A., Holleran, J., Wei, L., Hartwieg, E., Jorgensen, E. M. and Alfonso, A. (1999). UNC-11, a *Caenorhabditis elegans* AP180 homologue, regulates the size and protein composition of synaptic vesicles. *Mol. Biol. Cell* **10**, 2343-2360.

Orci, L., Malaisse-Lagae, F., Ravazzola, M., Amherdt, M. and Renold, A. E. (1973). Exocytosis-endocytosis coupling in the pancreatic beta cell. *Science* **181**, 561-562.

Rorsman, P. and Renstrom, E. (2003). Insulin granule dynamics in pancreatic beta cells. *Diabetologia* **46**, 1029-1045.

Rosenboom, H. and Lindau, M. (1994). Exo-endocytosis and closing of the fission pore during endocytosis in single pituitary nerve terminals internally perfused with high calcium concentrations. *Proc. Natl. Acad. Sci. USA* **91**, 5267-5271.

Rouze, N. C. and Schwartz, E. A. (1998). Continuous and transient vesicle cycling at a ribbon synapse. *J. Neurosci.* **18**, 8614-8624.

Sakmann, B. and Neher, E. (1995). Geometric parameters of pipettes and membrane patches. In *Single-channel Recording,* 2nd Edn (ed. B. Sakmann and E. Neher), pp. 637-650. New York: Plenem Press.

Scepek, S., Coorssen, J. R. and Lindau, M. (1998). Fusion pore expansion in horse eosinophils is modulated by Ca^{2+} and protein kinase C via distinct mechanisms. *EMBO J.* **17**, 4340-4345.

Schiavo, G., Gu, Q. M., Prestwich, G. D., Sollner, T. H. and Rothman, J. E. (1996). Calcium-dependent switching of the specificity of phosphoinositide binding to synaptotagmin. *Proc. Natl. Acad. Sci. USA* **93**, 13327-13332.

Schwake, L., Henkel, A. W., Riedel, H. D., Schlenker, T., Both, M., Migala, A., Hadaschik, B., Henfling, N. and Stremmel, W. (2002). Regulation of transferrin-induced endocytosis by wild-type and C282Y-mutant HFE in transfected HeLa cells. *Am. J. Physiol. Cell Physiol.* **282**, C973-C979.

Shields, M., La Celle, P., Waugh, R. E., Scholz, M., Peters, R. and Passow, H. (1987). Effects of intracellular Ca^{2+} and proteolytic digestion of the membrane skeleton on the mechanical properties of the red blood cell membrane. *Biochim. Biophys. Acta* **905**, 181-194.

Smillie, K. J. and Cousin, M. A. (2005). Dynamin I phosphorylation and the control of synaptic vesicle endocytosis. *Biochem. Soc. Symp.* **72**, 87-97.

Smith, R. M., Baibakov, B., Ikebuchi, Y., White, B. H., Lambert, N. A., Kaczmarek, L. K. and Vogel, S. S. (2000). Exocytotic insertion of calcium channels constrains compensatory endocytosis to sites of exocytosis. *J. Cell Biol.* **148**, 755-767.

Suss-Toby, E., Zimmerberg, J. and Ward, G. E. (1996). Toxoplasma invasion: the parasitophorous vacuole is formed from host cell plasma membrane and pinches off via a fission pore. *Proc. Natl. Acad. Sci. U.S.A* **93**, 8413-8418.

Takahashi, N., Kishimoto, T., Nemoto, T., Kadowaki, T. and Kasai, H. (2002). Fusion pore dynamics and insulin granule exocytosis in the pancreatic islet. *Science* **297**, 1349-1352.

Thomas, P., Lee, A. K., Wong, J. G. and Almers, W. (1994). A triggered mechanism retrieves membrane in seconds after Ca^{2+}-stimulated exocytosis in single pituitary cells. *J. Cell Biol.* **124**, 667-675.

Vogel, S. S., Smith, R. M., Baibakov, B., Ikebuchi, Y. and Lambert, N. A. (1999). Calcium influx is required for endocytotic membrane retrieval. *Proc. Natl. Acad. Sci. USA* **96**, 5019-5024.

von Gersdorff, H. and Matthews, G. (1994a). Dynamics of synaptic vesicle fusion and membrane retrieval in synaptic terminals. *Nature* **367**, 735-739.

von Gersdorff, H. and Matthews, G. (1994b). Inhibition of endocytosis by elevated internal calcium in a synaptic terminal. *Nature* **370**, 652-655.

Wendland, B. and Emr, S. D. (1998). Pan1p, yeast eps15, functions as a multivalent adaptor that coordinates protein-protein interactions essential for endocytosis. *J. Cell Biol.* **141**, 71-84.

Wendland, B., McCaffery, J. M., Xiao, Q. and Emr, S. D. (1996). A novel fluorescence-activated cell sorter-based screen for yeast endocytosis mutants identifies a yeast homologue of mammalian eps15. *J. Cell Biol.* **135**, 1485-1500.

Wu, L. G. (2004). Kinetic regulation of vesicle endocytosis at synapses. *Trends Neurosci.* **27**, 548-554.

Yang, S. D., Tallant, E. A. and Cheung, W. Y. (1982). Calcineurin is a calmodulin-dependent protein phosphatase. *Biochem. Biophys. Res. Commun.* **106**, 1419-1425.

Ye, W. and Lafer, E. M. (1995). Bacterially expressed F1-20/AP-3 assembles clathrin into cages with a narrow size distribution: implications for the regulation of quantal size during neurotransmission. *J. Neurosci. Res.* **41**, 15-26.

Zhang, B., Koh, Y. H., Beckstead, R. B., Budnik, V., Ganetzky, B. and Bellen, H. J. (1998). Synaptic vesicle size and number are regulated by a clathrin adaptor protein required for endocytosis. *Neuron* **21**, 1465-1475.